LAWRENCE
LIVERMORE
NATIONAL
LABORATORY

LLNL-JRNL-411835

Improvements to Regional Explosion Identification using Attenuation Models of the Lithosphere

M. E. Pasyanos, W. R. Walter

April 3, 2009

Geophysical Research Letters

Disclaimer

Improvements to Regional Explosion Identification using Attenuation Models of the Lithosphere

Michael E. Pasyanos, William R. Walter
Lawrence Livermore National Laboratory, Livermore CA

in preparation for Geophysical Research Letters

Abstract. Regional P/S amplitudes have been recognized as an effective discriminant between earthquakes and explosions. While closely spaced earthquake and explosions generally discriminate easily, the application of this technique to broad regions has been hampered by large variations in the amplitude of regional phases due to the attenuation structure of the crust and upper mantle. Making use of a recent P-wave and S-wave attenuation model of the lithosphere, we have found that correcting the events using our amplitude methodology significantly reduces the scattering in the earthquake population. We demonstrate an application of this technique to station NIL (Nilore, Pakistan) using broad area earthquakes and the 1998 Indian nuclear explosion recorded at the station using the Pn/Lg discriminant in the 1-2 Hz passband. We find that the explosion, which is lost in the scatter of the earthquakes in the uncorrected discriminant, clearly separates by correcting for the attenuation structure. We see a similar reduction in scatter and separation for the Pn/Sn and Pg/Lg discriminants in the same passband.

Introduction

Identifying underground nuclear explosions and discriminating them from a background of natural earthquakes is critical to the verification of nuclear test limitation agreements such as the Comprehensive nuclear-Test-Ban Treaty (CTBT). Earthquakes and explosions with closely located epicenters and recorded at the same station, show clear differences in their relative P-wave and S-wave amplitudes at high frequencies (usually > 3 Hz). These differences became apparent with the advent of widespread digital seismometry in the late 1980's and early 1990's, and have been documented by a large number of researchers at different test sites (e.g. Dysart and Pulli, 1987; Baumgardt and Young, 1990; Kim et al., 1993; Walter et al., 1995; Taylor, 1996; Hartse et al., 1997; Battone et al., 2002; Rodgers and Walter, 2002; Kim and Richards, 2007).

When earthquakes and explosions are nearly co-located, we can understand the observed seismic contrasts, such as the relative P-to-S wave excitation, in terms of depth, material property, focal mechanism and source time function differences. However, it is well known that path propagation effects (e.g. attenuation, blockage) can make earthquakes look like explosions. If the earthquake's initial S-wave amplitude is reduced below the signal's noise level due to such propagation effects, the resulting seismogram can look explosion-like based on its P/S ratio. To identify an explosion that does not have a nearby reference earthquake or more generally to compare P/S ratios for events over broad regions requires accounting for path effects.

In this study we make use of new crust and upper mantle attenuation maps to correct the regional phases for propagation effects over a broad region. We demonstrate that these maps allow explosion identification over broad areas. We apply the propagation corrections to earthquakes recorded at station NIL (Nilore, Pakistan). The station NIL was one of the few regional distance stations to record the May 11, 1998 Indian nuclear test. Previously Rodgers and Walter (2002) have demonstrated that P/S ratios discriminate this test from nearby earthquakes down to lower frequencies than usual, including the 1-2 Hz band where the new regional phase attenuation maps are available. Rodgers and Walter (2002) also showed that earthquakes to the north of NIL did not discriminate well using 1-2 Hz P/S ratio and simple one-dimensional path corrections. They achieved better results using a spatial correction technique based on Bayesian kriging (e.g. Schultz et al., 1998), but this still requires reference earthquakes in the vicinity of the explosion for proper identification. A major advantage of using tomography based attenuation maps is that no nearby reference events are required. In addition, using these maps does not preclude applying additional correction such as kriging when good reference events are available.

Regional Discrimination

Regional P/S discrimination relies on differences in the P-wave and S-wave generation of earthquakes and explosions. Earthquakes are well-modeled as slip on a plane and consequently are effective generators of both P-wave and S-wave energy. Nuclear explosions, on the other hand, are well-described as spherically symmetric pressure pulses, which theoretically generate only P-wave energy at the source. The sources of commonly observed explosion S-wave energy at frequencies below a few Hz have been the cause of much debate (e.g. Myers et al., 1999), and a variety of mechanisms such as the interaction with the free-surface, topography, rock damage, conversions at boundaries, and spall (e.g. Day and McLaughlin, 1991; Johnson and Sammis, 2001; Gupta and Patton, 2008; Vogfjord, 1997) have all been proposed to play a part. Despite the incomplete understanding of how the S-waves are generated, empirically the relative S-wave energy of explosions at sufficiently high frequencies is always observed to be significantly less than comparable-size tectonic earthquakes.

This can be readily seen where explosions occur in the vicinity of earthquakes. The top two waveforms in **Figure 1** show an explosion (in red) and a nearby earthquake (in green) recorded at the same station and filtered in the same passband (1-2 Hz). As compared to the explosion, the earthquake is rich is S-wave energy which propagates through the upper mantle (as Sn) and through the crust (as Lg). While the P/S discriminant would work well in this case, the challenge comes in monitoring broad regions. Like the explosion, the bottom waveform in **Figure 1a** (plotted in cyan) shows significant P-wave energy and small S-wave energy, making the waveform look explosion-like. However, this event is an earthquake. Although recorded at the same station using the same passband, the lack of S-waves is not caused by poor generation at the source, but rather path attenuation causing the low amplitudes of the Sn and Lg phases. Characterizing the path attenuation through attenuation tomography holds the

key to determining and correcting for the expected attenuation of phases along any given path through the region.

Attenuation Tomography

Recent work has focused on the attenuation of regional phases in the Middle East and vicinity and has been described thoroughly in several recent publications (Pasyanos et al., 2009a, 2009b). We will briefly summarize the method here and refer the reader to these earlier publications for details of the methodology. Like most amplitude tomography, we assume that the observed amplitudes are a product of four terms: the source term, the geometrical-spreading term, the attenuation term, and the site term. Our methodology, employed in Pasyanos et al. (2009a) for Lg, uses an MDAC source model (Walter and Taylor, 2001), which more explicitly defines the source expression in terms of an earthquake source model formulated in terms of the seismic moment. One of the advantages of this approach is to easily estimate the predicted Lg amplitudes for an event of any given location and size. We assume a geometrical spreading and provide parameters that relate the initial source term to the moment. Using amplitudes for about 6000 Lg paths, we then initialize the attenuation, site, and source terms and solve for all three sets of parameters in several different frequency bands.

In a subsequent paper (Pasyanos et al., 2009b), we applied the technique to simultaneously invert 1-2 Hz amplitudes of Pn, Pg, Sn and Lg to produce P-wave and S-wave attenuation models of the crust and upper mantle. The attenuation is modeled as P-wave and S-wave attenuation surfaces for the crust, and a similar set for the upper mantle. We can use all of the phase amplitudes together by using the appropriate (source, geometrical-spreading, site, and attenuation) terms for each phase. For example, the source terms of the P-waves and S-waves are different, and path attenuation is calculated by raypaths appropriate for the particular phase. Inverting all of the phases simultaneously (in this case, amplitudes for about 12,000 paths) allows us to determine consistent attenuation, site, and source terms for all phases, and eliminates non-physical inconsistencies among them. As a result, we can now predict the amplitudes of any of these regional phases for an event of any given location and size. **Figure 1b** shows the S-wave attenuation map of the crust in the 1-2 Hz passband for a portion of our study area. These crustal S-wave results are very similar to the 1-2 Hz Lg attenuation map in the earlier study (Pasyanos et al., 2009a). Attenuation is low (high Q) in northwest India / southeast Pakistan, eastern Kazakhstan, and Turkmenistan. Attenuation is high (low Q) in the north Indus Basin and west in Iran.

Results

P/S discriminants are expressed as the ratio between the P-wave amplitude (A^P) and the S-wave amplitude (A^S) and, because of the large variations, are usually plotted on a log scale. We examine the ratio of Pn amplitudes to Lg amplitudes in the 1-2 Hz passband recorded at station NIL in Nilore, Pakistan. Amplitudes employed in the discrimination analysis require a (pre-event) signal-to-noise ratio of 2.0 for P-waves and 1.3 for S-waves, with no additional pre-phase SNR criteria. This is in contrast to the pre-

event SNR of 2.0 and pre-phase SNR of 1.0 criteria used for all amplitudes in the attenuation tomography method. **Figure 2a** shows the ratio of the raw amplitudes as a function of distance. Besides the clear trend with distance (a result of the differing geometrical spreading and attenuation of the two phases), there is very large scatter in the earthquake population, which is due to a combination of factors, among them variations in path attenuation. Notice as well the Indian nuclear explosion of 11 May 1998 (plotted as a red star) falls within the scatter of the earthquakes, and the explosion cannot be reliably discriminated.

In order to correct the phase ratio for path and source effects, we adjust the individual amplitudes assuming an earthquake source. We then form our discriminant using the ratio of the corrected amplitudes. This is a division of the amplitudes or a subtraction in log-space:

$$\text{discriminant} = \log\left[\frac{(A^P/A_0^P)}{(A^S/A_0^S)}\right] = \log\left[\frac{A^P}{A^S}\right] - \log\left[\frac{A_0^P}{A_0^S}\right] \quad (1)$$

where A_0 are the amplitude predictions for an earthquake of that phase and size. As a result, the corrected discriminant should now have a value around 0 (P/S ratio of 1) for earthquakes. As in the attenuation tomography (Pasyanos et al., 2009a; 2009b), we input a best estimate of the earthquake size by using a moment magnitude, if available, or otherwise estimating Mw using other magnitude estimates.

The discriminant using corrected amplitudes is shown in **Figure 2b**. The trend with distance is now gone, the scattering of the earthquake population is reduced, and most importantly, the explosion separates cleanly from the earthquakes. Lg paths traversing regions of high crustal Q (e.g. to the south of NIL) will be normalized by high Lg amplitudes and hence have a higher P/S ratio. Those traversing regions of low crustal Q (e.g. to the north) will be normalized by low Lg amplitudes and have a lower P/S ratio.

It is important to note that in many areas where the lateral attenuation variations are low, we could correct the trends in distance and magnitude with a 1D correction. In this region, however, simply removing the trend would reduce the RMS of the earthquake population from 0.65 to 0.62 log-units, but the explosion would not separate from the earthquakes as the corrections would be the same for a given distance. Where lateral variations in attenuation are high, only 2D corrections can start to account for the large observed amplitude variations. After the attenuation corrections are applied, the RMS of the earthquake amplitude residuals reduces further to 0.37.

As seen in **Figure 2b**, there are still amplitude residuals, although greatly reduced from the raw amplitudes. At the shortest distances, we still see large residuals, as the attenuation model has only a small effect on these paths. The RMS ranges from ~0.4 log-units at distances less than 300 km, 0.3-0.4 log-units between 300 and 600 km epicentral distance, and < 0.3 log-units at distances greater than 600 km. These unmodelled amplitude variations can come from a number of possible sources, including small scale Q variations, variations in the source term (from seismic moment, apparent stress, depth,

etc.), differences in geometrical spreading, earthquake mislocations, and multipathing, to name a few. **Figure 3** shows residuals plotted on a map. While there seems to be some lateral variations in the residuals (higher values to the north and northeast; lower values to the west), there are larger variations within given geographic areas. Some variations (unmodelled Q, multipathing, apparent stress differences between shallow and deep earthquakes, poor moment estimates, mislocation effects), one might expect on short scales; others (regional stress, geometrical spreading) one might expect to be more regional.

Other regional P/S discriminants are used in instances where the Pn/Lg ratio might not be ideal. For example, in oceanic crust, the waveguide for Lg is blocked, and other suitable phase ratios would need to be employed. Other common regional P/S discriminants are: Pn/Sn and Pg/Lg, and we find a similar reduction in scatter and Indian nuclear test separation in the same passband (**Figure 4**), indicating that our attenuation model is predictive for all of the major regional phases.

Summary and Discussion

Making use of a recent attenuation model of the crust and upper mantle, we have found that correcting P-wave and S-wave amplitudes using the model significantly reduces the scattering in the P/S ratio and improves our discrimination ability. We demonstrate an application of this technique using broad area earthquakes and the 1998 Indian nuclear explosion recorded at station NIL using the Pn/Lg discriminant in the 1-2 Hz passband. We find that the explosion, which is lost in the scatter of the earthquakes in the uncorrected discriminant, clearly separates after correcting for the attenuation structure. We see a similar reduction in scatter and separation for other P/S discriminants in the same passband.

More generally, the ability to detect regional S-waves from earthquakes is key to P/S discrimination capability. If, for a particular source to station path, an explosion would have measureable high frequency S-waves, its relatively high P/S ratio can be a solid discriminant. If, instead, only an earthquake would have detectable S-waves, but not a similar sized explosion, there is still some discrimination potential using P/S. If, however, even an earthquake of that size would not have detectable S-waves, then there is no P/S discrimination potential. Our attenuation modeling can provide the necessary tools to estimate discrimination capability of regional P/S amplitudes for particular paths as a function of magnitude and frequency.

We plan to further test the ability of attenuation models to improve P/S discrimination for other datasets of earthquake and explosions. While we have every expectation that this method and our attenuation model should work well over broad regions, the challenge will be to calibrate attenuation structure at higher frequencies where the P/S discriminant works better, but where data coverage for tomographic modeling is sparser.

Acknowledgments. We would especially like to thank Eric Matzel for making many of the amplitude measurements used in the attenuation tomography. This work was

performed under the auspices of the U.S. Department of Energy by Lawrence Livermore National Laboratory under Contract DE-AC52-07NA27344. This is LLNL contribution LLNL-JRNL-******.

References

Battone, S., M.D. Fisk and G.D. McCarter (2002). Regional seismic-event characterization using a Bayesian formulation of simple kriging, Bull. Seism. Soc. Am., 92, 2277-2296.

Baumgardt, D.R. and G.B. Young (1990). Regional seismic waveform discriminants and case-based identification using regional arrays, Bull. Seism. Soc. Am., 80, 1874-1892.

Day, S. and K. McLaughlin (1991). Seismic Source Representations for Spall, Bull. Seism. Soc. Am. 81, 191-201.

Dysart, P.S. and J.J. Pulli (1987). Spectral study of regional earthquakes and chemical explosions recorded at the NORES array. SAIC technical report C87-03.

Gupta, I.N. and H.J. Patton (2008). Difference spectrograms: a new method for studying S-wave generation from explosions, Bull. Seism. Soc. Amer., 98, 2460-2468, DOI: 10.1785/0120080057.

Hartse, H., S.R. Taylor, W.S. Phillips, and G.E. Randall (1997). A preliminary study of regional seismic discrimination in Central Asia with an emphasis on Western China, Bull. Seism. Soc. Am. 87, 551-568.

Johnson, L.R. and C.G. Sammis (2001). Effects of rock damage on seismic waves generated by explosions, Pure Appl. Geophys., 158, 1869-1908

Kim, W.-Y., D.W. Simpson, and P.G. Richards (1993). Discrimination of earthquakes and explosions in the eastern United States using regional high frequency data, Geophys. Res. Lett., 20, 1507-1510.

Kim, W.-Y., and P.G. Richards (2007). North Korean nuclear test: seismic discrimination at low yield, EOS, 88, 157-161.

Myers, S.C., W.R. Walter, K. Mayeda, and L. Glenn (1999). Observations in support of Rg scattering as a source for explosion S waves: regional and local recordings of the 1997 Kazakhstan depth of burial experiment, Bull. Seismol. Soc. Am., 89, 544-549.

Pasyanos, M.E., E.M. Matzel, W.R. Walter, and A.J. Rodgers (2009a). Broadband Lg Attenuation Modeling of the Middle East, in press Geophys. J. Int., doi: 10.1111/j.1365-246X.2009.04128.x

Pasyanos, M.E., W.R. Walter, and E.M. Matzel (2009b). A simultaneous multi-phase approach to determine P-wave and S-wave attenuation of the crust and upper mantle, submitted to Bull. Seism. Soc. Amer.

Rodgers, A.J. and W.R. Walter (2002). Seismic discrimination of the May 11, 1998 Indian nuclear test with short-period regional data from Station NIL (Nilore, Pakistan), Pure Appl. Geophys. 159, 4, 679-700, DOI - 10.1007/s00024-002-8654-6

Schultz, C., S. Myers, J. Hipp, and C. Young (1998). Nonstationary Bayesian kriging: a predictive technique to generate corrections for detection, location, and discrimination, Bull. Seism. Soc. Am. 88, 1275–1288.

Taylor, S. (1996). Analysis of high-frequency Pg/Lg ratios from NTS explosions and Western U.S. earthquakes, Bull. Seism. Soc. Am., 86, 1042-1053.

Taylor, S., A. Velasco, H. Hartse, W.S. Philips, W.R. Walter, and A. Rodgers (2002). Amplitude corrections for regional discrimination, Pure. App. Geophys. 159, 623-650.

Vogfjord, K. (1997). Effect of explosion depth and earth structure on the excitation of Lg waves: S* revisited, Bull. Seism. Soc. Am. 87, 1100-1114.

Walter, W.R., K. Mayeda, and H.J. Patton (1995). Phase and spectral ratio discrimination between NTS earthquakes and explosions Part 1: Empirical observations, Bull. Seism. Soc. Am., 85., 1050-1067.

Walter, W.R. and S.R. Taylor (2001). A revised magnitude and distance amplitude correction (MDAC2) procedure for regional seismic discriminants: theory and testing at NTS, Lawrence Livermore National Laboratory, UCRL-ID-146882 http://www.llnl.gov/tid/lof/documents/pdf/240563.pdf

Figure captions

Figure 1. a) Waveforms of two earthquakes (shown in green and cyan) and one nuclear explosion (shown in red) recorded at station NIL and filtered between 1-2 Hz. b) Shear-wave attenuation of the crust from amplitude topography of regional phases. This map is primarily sensitive to the attenuation of the crustally-propagating shear-wave Lg. Black triangle is station NIL, red star the 1998 Indian nuclear explosion, and circles the earthquakes near the Indian test (green) and in Kyrgyzstan (cyan).

Figure 2. Pn/Lg discriminant at 1.0-2.0 Hz frequency recorded at station NIL showing a) raw data and b) data with attenuation corrections. The plot shows log(Pn/Lg) as a function of distance (in km). Blue circles are earthquakes and the red star is the 1998 Indian nuclear explosion. The green circle is the earthquake just north of the Indian test

shown in Figure 1a, and the cyan circle is the Kyrgyz earthquake also shown in Figure 1a.

Figure 3. Pn/Lg residuals plotted on a map of the region. Colored circles are earthquakes and the star the 1998 Indian nuclear explosion. Large circles outline epicentral distances of 200 km and 1600 km from station NIL (black triangle).

Figure 4. a) Pn/Sn discriminant at 1.0-2.0 Hz frequency recorded at station NIL showing data with attenuation corrections. b) Pg/Lg discriminant at 1.0-2.0 Hz frequency recorded at station NIL showing data with attenuation corrections. The plots show log(Pn/Lg) as a function of distance (in km). Symbols the same as in Figure 2.

a)

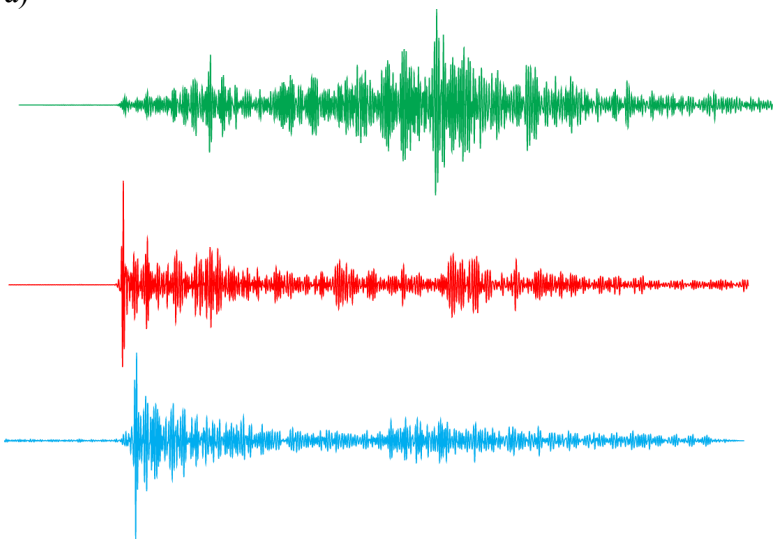

b)

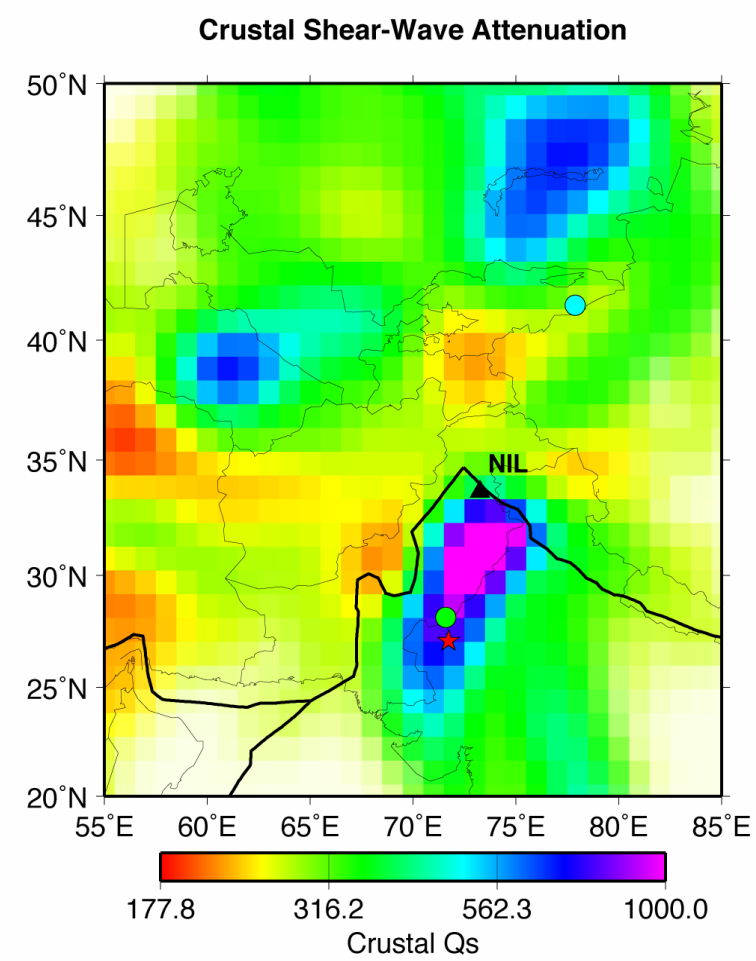
Crustal Shear-Wave Attenuation
50˚N
45˚N
40˚N
35˚N
30˚N
25˚N
20˚N
NIL
55˚E
60˚E
65˚E
70˚E
75˚E
80˚E
85˚E
177.8
316.2
562.3
1000.0
Crustal Qs

Figure 1.

337 a) b)

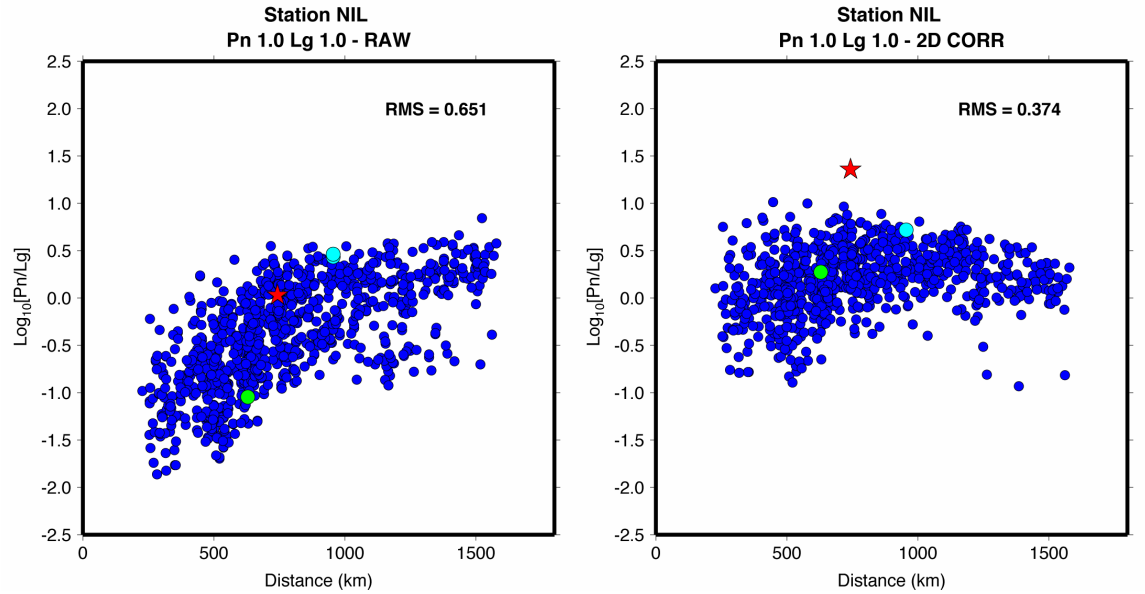

338
339

340 Figure 2.

341

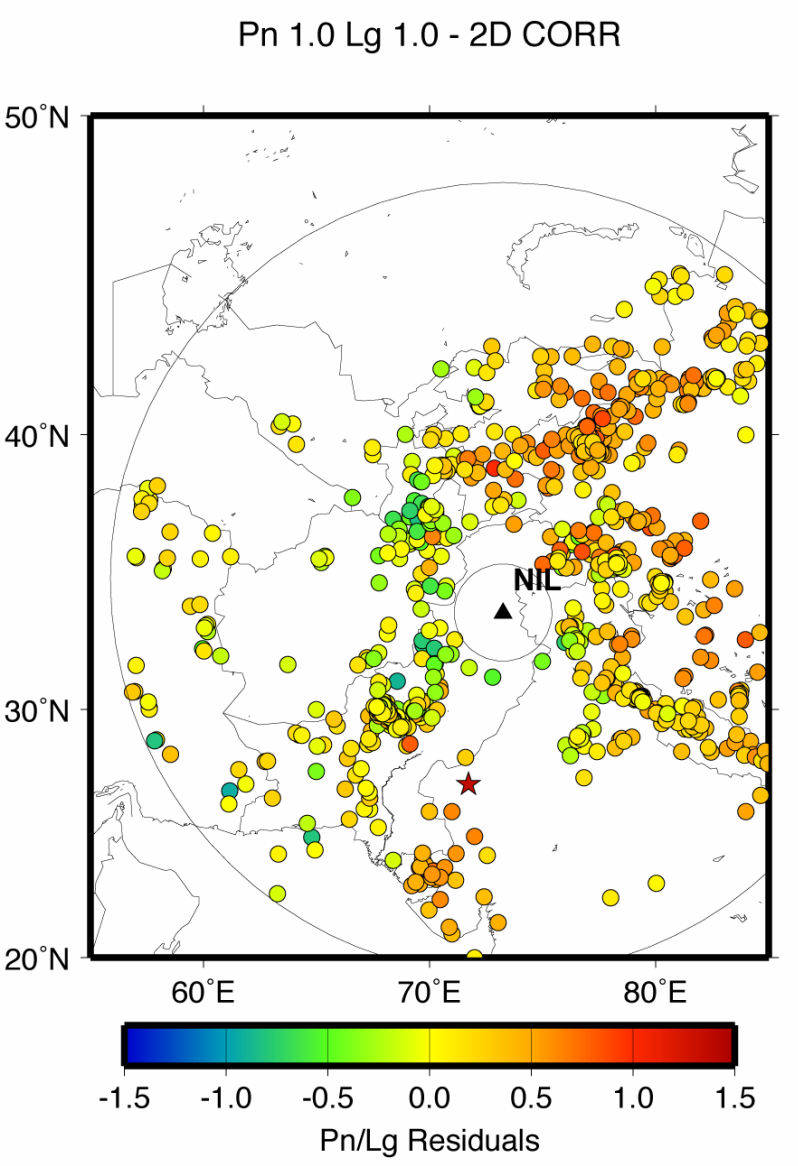
Pn 1.0 Lg 1.0 - 2D CORR
50˚N
40˚N
30˚N
20˚N
60˚E
70˚E
80˚E
NIL
-1.5
-1.0
-0.5
0.0
0.5
1.0
1.5
Pn/Lg Residuals

Figure 3.

a) b)

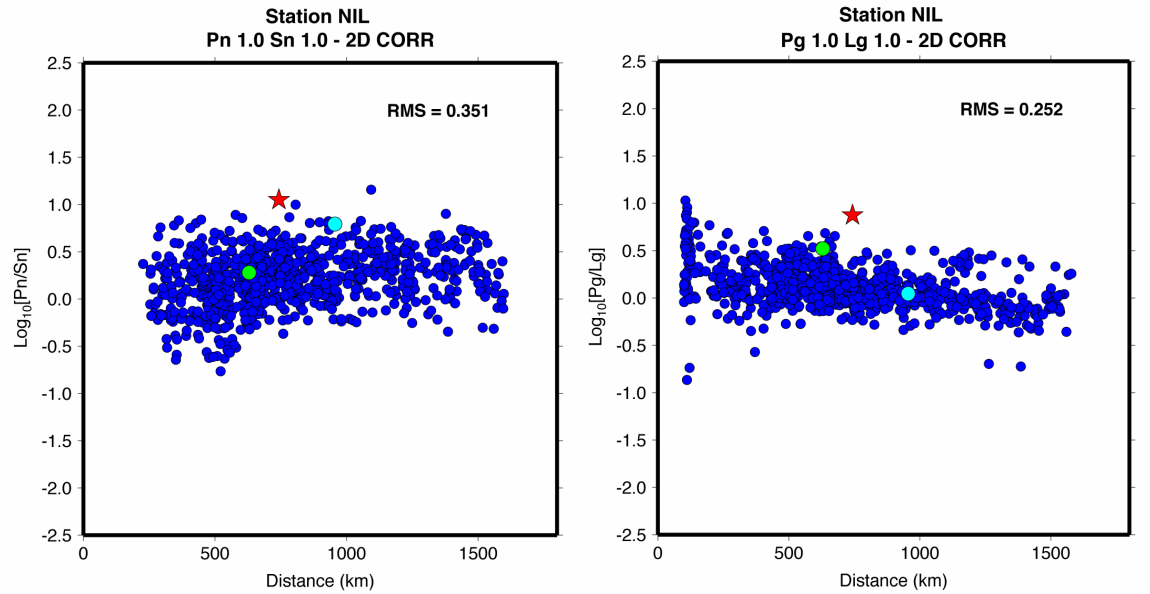
Station NIL
Pn 1.0 Sn 1.0 - 2D CORR
RMS = 0.351
Log10[Pn/Sn]
Distance (km)
Station NIL
Pg 1.0 Lg 1.0 - 2D CORR
RMS = 0.252
Log10[Pg/Lg]
Distance (km)

Figure 4.